Performance of Instantaneous Frequency Rate Estimation Using High-Order Phase Function

Pu Wang, Hongbin Li, Igor Djurović, and Braham Himed

Abstract— **The high-order phase function (HPF) is a useful tool to estimate the instantaneous frequency rate (IFR) of a signal with a polynomial phase. In this paper, the asymptotic bias and variance of the IFR estimate using the HPF are derived in closed-forms for the polynomial phase signal with an arbitrary order. The Cramér-Rao bounds (CRBs) for IFR estimation, in both exact and asymptotic forms, are obtained and compared with the asymptotic mean-square error (MSE) of the HPF-based IFR estimator. Simulations are provided to verify our theoretical results.**

I. Introduction

Polynomial phase structure has been widely used to model nonstationary signals appearing in radar, sonar, communications, and passive acoustic applications [1, 2]. A pth-order polynomial phase signal (PPS) is given by

$$s(t) = Ae^{\{j\phi(t)\}} = Ae^{\left\{ j \sum_{i=0}^{p} a_i t^i \right\}}, \qquad (1)$$

where A is the constant amplitude, $\phi(t)$ is the instantaneous phase (IP) and $\{a_i\}_{i=0}^{p}$ are unknown phase parameters, respectively. While the instantaneous frequency (IF) is the first derivative of the IP, the instantaneous frequency rate (IFR) is defined as the second derivative of the IP [3], i.e.,

$$\Omega(t) = \frac{d^2\phi(t)}{dt^2} = \sum_{i=2}^{p} i(i-1)a_i t^{i-2}, \qquad (2)$$

where $\Omega(t)$ denotes the IFR of the signal in (1). When $p = 2$, i.e., a linear FM signal, the IFR reduces to the well known chirp-rate, i.e., $\Omega(t) = 2a_2$ [4]. In practice, the IFR could reveal the rate-of-change of the velocity, i.e., acceleration, of a moving target.

IFR estimation is a frequently encountered task in radar applications. In synthetic aperture radar (SAR), echoes are often modeled by incorporating time-varying acceleration [5, 6]. Target acceleration was shown to affect the SAR ground moving-target indication in [7] and [8], where compensation techniques were also examined. IFR can be estimated by using a polynomial Fourier transform [9]. The resulting estimator, however, requires a computationally intensive multi-dimensional search [9]. This motivated later efforts to search for more efficient solutions. A notable example is the cubic phase function (CPF) based estimator [3], which requires only a one-dimensional search. The CPF was originally introduced to estimate the IFR of a quadratic FM signal. Extension of the CPF led to the high-order phase function (HPF) [10], which can be used to estimate the IFR of a high-order PPS. The asymptotic performance of the CPF-based IFR estimate for the quadratic FM signal was derived in [10]. However, similar analysis for the HPF-based IFR estimator of a general PPS is unavailable.

In this paper, a unified analysis of the HPF-based IFR estimator for a PPS with an *arbitrary* order is presented. The asymptotic bias and variance of the HPF-based IFR estimate are derived in closed-form at high Signal to Noise Ratio (SNR) by using a first-order perturbation analysis. It is shown that the HPF-based IFR estimator is asymptotically unbiased and its asymptotic variance is a function of the SNR, time and the HPF coefficients (see Section III for an explanation). Our results are consistent with that derived in

IEEE Transactions on Signal Processing, Vol. 58, No. 4, Apr. 2010.

[3] and [10] for the case of $p = 3$. Furthermore, since multiple forms of the HPF exist for the analysis of a given PPS, our results can be used to predict their performance and provide guideline on how to choose a proper HPF for the problem at hand. On the other hand, to establish a performance benchmark for all (asymptotically) unbiased IFR estimators, the Cramér-Rao bounds (CRBs) for IFR estimation, in both exact and asymptotic forms, are presented in closed-form. The CRB shows a dependence on the PPS order, the number of samples, time and SNR. Performance comparison between the HPF-based estimators and the high-order ambiguity function (HAF)-based method [11] is also presented.

The rest of this paper is organized as follows. The HPF is first reviewed in Section II. Section III outlines the derived expressions for the asymptotic bias and mean-squared error (MSE). The CRB for IFR estimation is also derived. Section IV provides simulation results to verify our theoretical analysis. Finally, conclusions are provided in Section V.

II. High-order Phase Function

For a pth-order PPS defined in (1), the HPF, specified by $H_q(t,\omega)$, was defined by using a high-order nonlinear kernel $K_q(t,\tau)$ as [10]

$$K_q(t,\tau) = \prod_{l=1}^{q/2} \left[s(t+d_l\tau)s(t-d_l\tau)\right]^{(r_l)},$$
$$H_q(t,\omega) = \int_{-\infty}^{+\infty} K_q(t,\tau)e^{-j\omega\tau^2}d\tau, \tag{3}$$

where $\mathbf{d} \triangleq \left\{\mathbf{d_1}, \mathbf{d_2}, \cdots, \mathbf{d_{q/2}}\right\}$ denotes a set of lag-coefficients, $\mathbf{r} \triangleq \left\{\mathbf{r_1}, \mathbf{r_2}, \cdots, \mathbf{r_{q/2}}\right\}$ is used to impose complex conjugation if $r_i = 1$, and ω denotes the index in the IFR domain. From (3), it is seen that the HPF has a qth-order nonlinearity due to the $q/2$ consecutive bilinear transformations. If $q = 2, d_1 = 1$ and $r_1 = 1$, the $H_2(t,\omega)$ reduces to the CPF in [3].

In the noisy-free case, assume the kernel is selected such that

$$K_q(t,\tau) = A^q e^{j\tau^2\Omega(t)+j\varsigma}, \tag{4}$$

where ς is a term independent of τ, the squared magnitude of the HPF is centered on the IFR due to the match filtering in (3). To meet (4), the HPF coefficients should satisfy [12]

$$\sum_{l=1}^{q/2} r_l d_l^2 = 1,$$
$$\sum_{l=1}^{q/2} r_l d_l^m = 0, \text{ for even values of } m\text{: } 4 \le m \le p. \tag{5}$$

Therefore, for any given time, e.g., $t = t_s$, the IFR $\Omega(t_s)$ can be estimated by searching for the maximum of $|H_q(t_s,\omega)|^2$ over ω.

For a given PPS, there may exist more than one real solution to the set of equations in (5). For example of a quadratic FM signal ($p = 3$), we have at least two choices satisfying (5)

$$H_2(t,\omega) = \int_{-\infty}^{+\infty} s(t+\tau)s(t-\tau)e^{-j\omega\tau^2}d\tau, \tag{6}$$

$$H_4(t,\omega) = \\ = \int_{-\infty}^{+\infty} s^2\left(t+\frac{\sqrt{2}}{2}\tau\right)s^2\left(t-\frac{\sqrt{2}}{2}\tau\right)e^{-j\omega\tau^2}d\tau. \tag{7}$$

One immediate question arising from the above discussion is the choice of the solution for the problem at hand. A natural choice to select a proper form of HPF is the performance of the estimator including the bias, the MSE, and the SNR threshold, which will be discussed later.

III. Performance of the HPF-based IFR Estimator

Consider a noise-corrupted PPS

$$x(n) = Ae^{j\sum_{i=0}^{p} a_i n^i} + v(n), \quad n = 0, 1, ..., N-1, \tag{8}$$

where $x(n)$ denotes the nth sample of the noisy observations, $v(n)$ is an additive complex white Gaussian noise with zero mean and variance σ^2, and N is the number of samples. It should be noted that, while condition (5) ensures the unbiased IFR estimate in the absence of noise, the unbiased property does not automatically carry over the case with observation noise.

The discrete HPF (c.f. (3)) for the noisy PPS can be decoupled to

$$H_x(n,\omega) = \sum_{m=-M}^{M} \left[K_s(n,m) + K_v(n,m)\right] e^{-j\omega m^2}, \tag{9}$$

where $K_s(n,m)$ and $K_v(n,m)$ represent the signal and noise components, respectively, $2M+1$ is the length of a two-sided window. For simplicity, we use ω in both continuous and discrete cases.

Appendix A shows that, at high SNR, the signal component $K_s(n,m)$ and the noise component $K_v(n,m)$ can be approximated by ignoring the high-order noise terms [13]

$$\begin{aligned} K_s(n,m) &= \prod_{i=1}^{L} \left[s(n+d_i m)s(n-d_i m)\right]^{(r_i)k_i}, \\ K_v(n,m) &\approx K_s(n,m) \left(\sum_{i=1}^{L} k_i \left[\frac{v^{(r_i)}(n+d_i m)}{s^{(r_i)}(n+d_i m)} \right.\right. \\ &\quad \left.\left. + \frac{v^{(r_i)}(n-d_i m)}{s^{(r_i)}(n-d_i m)} \right] \right). \end{aligned} \tag{10}$$

where L is the number of distinct HPF coefficient pairs (d_i, r_i), k_i is the multiplicity of the ith HPF coefficient pair (d_i, r_i), and $\sum_{i=1}^{L} k_i = q/2$. From (10), it is seen that $K_s(n,m)$ contains only signal-related terms and therefore is deterministic, whereas $K_v(n,m)$ includes interacting signal-and-noise terms which are random. More specifically, $K_v(n,m)$ acts like a random perturbation which moves the maximum of the HPF, denoted as $\omega_0 = \Omega(n)$, by a random amount $\delta\omega$, which results in a deviated IFR estimate $\hat{\omega} = \omega_0 + \delta\omega$. The performance analysis is to quantify the first- and second-order statistics, i.e., the bias and variance, of the random error $\delta\omega$. A first-order perturbation analysis [14], which is repeated in Appendix B, is utilized. A detailed analysis of the random estimate error $\delta\omega$ using the first-order perturbation is presented in Appendix C, and the results are summarized as follows.

A. Asymptotic Bias and Variance of the HPF-based Estimator

Proposition 1: For a pth-order noisy PPS, the asymptotic bias and variance of the HPF-based IFR estimator at high SNR are given by:

$$\begin{aligned} &E\{\delta\omega\} = 0, \\ &E\left\{(\delta\omega)^2\right\} = \\ &= \frac{90 \sum_{i=1}^{L} k_i^2}{\mathrm{SNR} M(M+1)(2M+3)(4M^2-1)}, \end{aligned} \tag{11}$$

where the SNR is defined as A^2/σ^2.

From *Proposition 1*, the HPF-based IFR estimator is asymptotically unbiased, and the variance of the estimation error, which is also the MSE in this case, is independent of the phase parameter $\{a_i\}_{i=0}^{p}$. On one hand, the MSE is proportional to the sum of the squared multiplicity of the HPF coefficients. On the other hand, the asymptotic MSE is inversely proportional to the SNR and M^5. The larger the window length, the lower the MSE. As such, for a given SNR and time n, the minimum MSE is achieved by using the maximum window length, which leads to the following proposition.

Proposition 2: For a fixed SNR and N, the minimum MSE of the HPF-based IFR estimator at time n is given by

$$E\left\{(\delta\omega)^2\right\} \approx \frac{45 \sum_{i=1}^{L} k_i^2}{4\mathrm{SNR} M_{\max}^5(n,N,\mathbf{d})}, \tag{12}$$

where the maximum window length at time n is given by

$$M_{\max}(n,N,\mathbf{d}) = \left\lfloor \frac{\min\{\mathbf{n}, \mathbf{N-1-n}\}}{\max\{\mathbf{d}\}} \right\rfloor, \tag{13}$$

with $\lfloor\cdot\rfloor$ denotes the floor function, since $0 \le n \pm \max\{\mathbf{d}\} M_{\max} \le N-1$. From *Proposition 2*, the minimum MSE of the IFR estimator at time n is determined by the SNR, the number of samples, time instant, and the HPF coefficients $\mathbf{d}$. Note that the MSE is also a function of the HPF order q through L and k_i since $\sum_{i=1}^{L} k_i = q/2$, and is further dependent on the PPS order p due to (5).

B. Cramér-Rao Bounds for IFR Estimation

The achievable accuracy of any (asymptotically) unbiased IFR estimator can be identified by means of the CRB. To this end, we derive the CRBs for IFR estimation in both exact and asymptotic forms.

B.1 Exact CRB

The CRB for estimating the phase parameter $\mathbf{a} \triangleq [\mathbf{a_0}, \mathbf{a_1}, \cdots, \mathbf{a_p}]^{\mathbf{T}}$ was carried out in [15]. Of interest to us is the CRB for IFR estimation, not for the phase parameter $\mathbf{a}$. Note, however, that the IFR of the PPS is a function of $\mathbf{a}$ and time n as $\Omega(n) = \mathbf{a^T t}$, where $\mathbf{t} \triangleq \left[\mathbf{0}, \mathbf{0}, \mathbf{2}, \cdots, \mathbf{p}\left(\mathbf{p}-\mathbf{1}\right)\mathbf{n^{p-2}}\right]^{\mathbf{T}}$. By applying the transformation rule for the CRB (see Appendix 3B of [16]) and noting that the above function is a $(p+1)$-dimensional-to-scalar transformation, we have

$$\mathrm{var}\left(\hat{\omega}\right) \geq \frac{\sigma^2}{2A^2}\mathbf{t}\mathbf{H}_{\mathbf{p+1}}^{-\mathbf{1}}\mathbf{t}^{\mathbf{T}}. \tag{14}$$

where $\mathbf{H_{p+1}}$ is defined in (18) of [15]. With results on the inverse of $\mathbf{H_{p+1}}$ (see (22)-(33) of [15]), (14) can further be expressed

$$\mathrm{var}\left(\hat{\omega}\right) \geq \frac{\sigma^2}{2A^2 N}\mathbf{t}\mathbf{E}_{\mathbf{p+1}}^{-\mathbf{1}}\mathbf{B}_{\mathbf{p+1}}\mathbf{E}_{\mathbf{p+1}}^{-\mathbf{1}}\mathbf{t}^{\mathbf{T}}, \tag{15}$$

where $\mathbf{E_{p+1}}$ and $\mathbf{B_{p+1}}$ are defined in (24) and (32) of [15]. From (15), it is not clear how the coefficients (e.g., p, n, N) affect the CRB. In the following, we show how the CRB depends on these coefficients under the assumption of large samples.

B.2 Asymptotic CRB for Large N

For large N (i.e., $N \gg p$), noting that

$$\frac{1}{\iota+\kappa+1} \gg \frac{(p+1)^2}{2N(\iota+1)(\kappa+1)} - \frac{1}{2N},$$

$$2 \leq \iota, \kappa \leq p, N \gg p,$$

in the expression of $\mathbf{B_{p+1}}$, we derive an asymptotic CRB.

Proposition 3: For a noisy pth-order PPS, the asymptotic variance of any unbiased IFR estimator is bounded by

$$\mathrm{var}\left(\hat{\omega}\right) \geq \frac{1}{2\mathrm{SNR}}\sum_{k=0}^{2p-4} C_p(k)\frac{n^k}{N^{(k+5)}}, \tag{16}$$

where

$$C_p(k) = \sum_{\substack{2 \leq \iota, \kappa \leq p \\ \iota+\kappa-4=k}} c_p(\iota,\kappa) \tag{17}$$

with

$$c_p(\iota,\kappa) =$$
$$= (-1)^{\iota+\kappa}\frac{\iota\kappa(\iota-1)(\kappa-1)(p+\iota+1)(p+\kappa+1)}{\iota+\kappa+1}$$
$$\times \begin{pmatrix} p+\iota \\ \iota \end{pmatrix}\begin{pmatrix} p \\ \iota \end{pmatrix}\begin{pmatrix} p+\kappa \\ \kappa \end{pmatrix}\begin{pmatrix} p \\ \kappa \end{pmatrix}.$$

Remark: The above CRB is for the asymmetric sampling case $n = 0, \cdots, N-1$. It can be extended to the symmetric sampling case $n = -(N-1)/2, \cdots, (N-1)/2$. According to [17], it can be shown that the asymptotic CRB for IFR estimation in the asymmetric sampling case is

$$\mathrm{var}\left(\hat{\omega}\right) \geq \frac{1}{2\mathrm{SNR}}\sum_{k=0}^{2p-4} C_p(k)\frac{\left(n+\frac{N-1}{2}\right)^k}{N^{(k+5)}}. \tag{18}$$

Note that the coefficients $C_p(k)$ are a function of p only and hence can be computed in advance for any given PPS order. Table I shows the values of $C_p(k)$ for the PPS with order $p \leq 4$. Moreover, the asymptotic CRB in (16) is a $(2p-4)$th-order polynomial in n with coefficient $C_p(k)/\left(2\mathrm{SNR}N^{k+5}\right)$ for the kth item in n. This polynomial phenomenon is analogous to the polynomial structure of the IFR in n (see (2)) where the kth term n^k is associated with a^{k+2} whose CRB is inversely proportional to the SNR and N^{2k+5}.

The accuracy of approximating (15) with (16) is examined at the middle point of observations in the cases of $p = 4$ and $p = 6$ when SNR = 10 dB in Figure 1. It is seen that our large sample approximation works fine even for small N. For $N \geq 100$, the approximation makes no difference between the two CRBs.

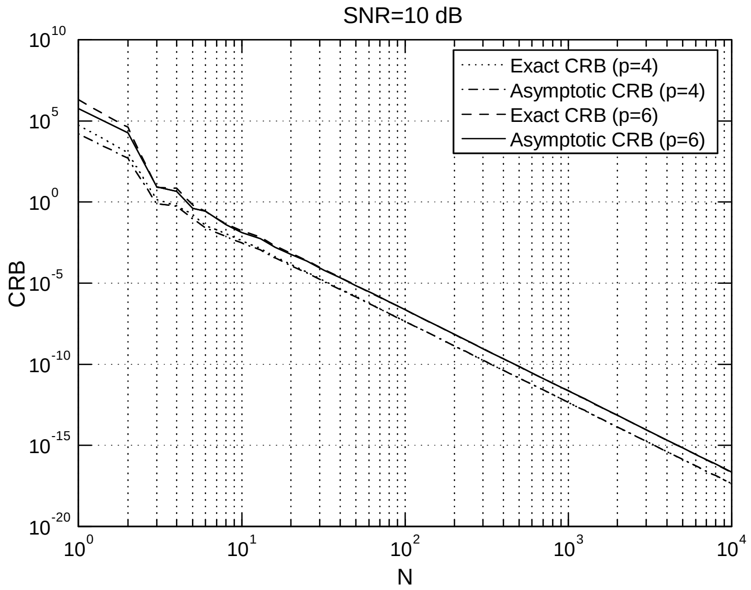

Fig. 1. Exact and asymptotic CRBs versus the number of samples N.

TABLE I
VALUES OF $C_p(k)$ FOR THE PPS WITH ORDER $p \leq 4$

p	$k=0$	$k=1$	$k=2$	$k=3$	$k=4$
2	720				
3	25920	-100800	100800		
4	317520	-2822400	9172800	-12700800	6350400

C. Examples

In general, the above results on the variance of the HPF-based IFR estimate and the CRB for IFR estimation are valid for any PPS with an order p. Nevertheless, links to two simple cases of $p = 2$ and $p = 3$ are useful to illustrate our analytical results.

Linear FM Signal ($p = 2$): The IFR reduces to $\Omega(n) = 2a_2$, and the CRB for IFR estimation is

$$\mathrm{CRB}\left\{\Omega\right\} = \frac{360}{N^5\mathrm{SNR}}. \tag{19}$$

Using the transformation rule of the CRB [16, Section 3.6], this result is effectively the same as the CRB for a_2 of the linear FM signal (see (33) of [14]) by a factor of 4 since $\Omega(n) = 2a_2$.

When H_2 in (6) is used, the MSE of the IFR estimate in (11) at the middle point from (12) is

$$E\left\{(\delta\omega)^2\right\} \approx \frac{360}{N^5\mathrm{SNR}}, \tag{20}$$

which is consistent with the MSE of the H_2-based a_2 estimate at the middle point by a factor of 4 [12, Appendix-A].

Quadratic FM Signal ($p = 3$): From (16), the CRB for IFR estimation is a function of n, SNR, and N:

$$\mathrm{CRB}\left\{\Omega\right\} = \frac{12960}{N^5\mathrm{SNR}} - \frac{50400}{N^6\mathrm{SNR}}n + \frac{50400}{N^7\mathrm{SNR}}n^2. \tag{21}$$

As discussed above, the CRB is a second-order polynomial in n.

As shown in [10], H_2 can be used to estimate the IFR of the quadratic FM signal. In this case, the MSE in (11) reduces to

$$E\left\{(\delta\omega)^2\right\} \approx \frac{45}{4M^5\mathrm{SNR}}. \tag{22}$$

To connect our results to [10], we notice that the maximum window length of H_2 at time n is $M_{\max} = N/2 - |n|$ for the case $-(N-1)/2 \leq n \pm m \leq (N-1)/2$, as considered in [10]. Therefore, the minimum MSE of the H_2-based IFR estimate at n is

$$E\left\{(\delta\omega)^2\right\} \approx \frac{45}{4\left(\frac{N}{2} - |n|\right)^5 \mathrm{SNR}}, \tag{23}$$

which coincides with (40) of [10] at high SNR.

IV. Simulation Results

In the following, we consider two numerical examples to verify our analytical results. All simulated results are based on 300 Monte-Carlo simulations. For the HPF-based methods, interpolation is used whenever the lag-coefficient is not an integer.

A. Quadratic FM Signal

For a quadratic FM signal, both H_2 and H_4 can be applied to estimate the IFR. According to *Proposition 1*, the asymptotic MSEs for both estimates are

$$E\left\{(\delta\omega)^2\right\}_{H_2} \approx \frac{45}{4M^5\mathrm{SNR}},$$
$$E\left\{(\delta\omega)^2\right\}_{H_4} \approx \frac{45}{M^5\mathrm{SNR}}.$$

To verify our analytical results, a quadratic FM signal with parameters $A = 1$, $(a_0, a_1, a_2, a_3) = \left(1, \pi/8, 5\times10^{-3}, 10^{-5}\right)$, and $N = 129$ is generated. Fig. 2 shows the simulated MSE at $n = 64$ (i.e., the middle point of observations) by using H_2, H_4 and the HAF when the SNR varies from -5 dB to 15 dB. The length of window is $M = 64$. From this figure, we have the following observations:

1. At high SNR, the simulated MSEs for both H_2 and H_4 agree with their own theoretical results. Note that the theoretical and simulated MSEs of the H_2 attain the CRB when the SNR is above 1 dB. The MSEs of the H_4-based estimate are about four times higher than the H_2-based and HAF-based MSEs when the SNR is greater than 6 dB.
2. The H_4 and the HAF show a higher SNR threshold than the H_2 because the former two involve a fourth-order nonlinearity while the H_2-based method has only a second-order nonlinearity. In this example, the SNR threshold for the H_4 and the HAF is about 6 dB, whereas the H_2 exhibits a threshold at around 2 dB. Note that nonlinear estimators usually exhibit a threshold effect (see Chapter 7 of [16]).

The variation of the MSE as a function of n is shown in Fig. 3 when $N = 129$ and $\mathrm{SNR} = 10$ dB. At each time point n, we use the window length $M = \min\{n, N-1-n\}$. Both the MSE and CRB are seen to be symmetric with respect to the middle point $n = 64$. The numerical results are seen to agree with the theoretical results. Again, the H_2-based estimator shows lower MSEs than those of the H_4-based estimator. In general, for a quadratic FM signal, the H_2-based estimator provides the best performance in terms of MSEs and the SNR threshold among various HPFs.

B. Cubic FM Signal

For a cubic FM signal ($p = 4$), the minimum HPF order is $q = 6$ due to (5). By minimizing the theoretical MSE in *Proposition 2* with subject to (5), we can numerically determine the sixth-order HPF with the minimum MSE as H_6 with $\mathbf{r} = (\mathbf{1}, \mathbf{1}, -\mathbf{1})$ and $\mathbf{d} = (\mathbf{1.2646}, \mathbf{1.3544}, \mathbf{1.5600})$. For comparison purposes, we also consider two other HPFs: (1) H_6' with $\mathbf{r} = (\mathbf{1}, \mathbf{1}, -\mathbf{1})$ and $\mathbf{d} = (\mathbf{1.0875}, \mathbf{1.9333}, \mathbf{1.9800})$, and (2) H_8 with $\mathbf{r} = (\mathbf{1}, \mathbf{1}, -\mathbf{1}, -\mathbf{1})$ and $\mathbf{d} = (\mathbf{1.4759}, \mathbf{2.9432}, \mathbf{2.9800}, \mathbf{0.9800})$. Their theoretical MSEs can easily be obtained from *Proposition 2* and will be compared in the following simulations.

To verify our analytical results, a cubic FM signal with parameters $A = 1$, $(a_0, a_1, a_2, a_3, a_4) = \left(1, \pi/8, 3\times10^{-4}, 2.5\times10^{-7}, 10^{-10}\right)$, and $N = 129$ is generated. Fig. 4 shows the theoretical and simulated MSEs for the three HPFs and the HAF as a function of the SNR when

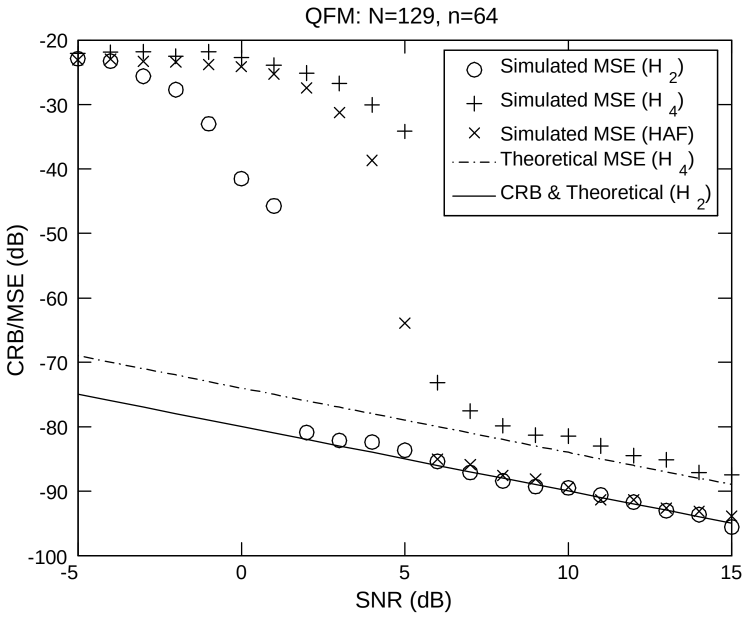

Fig. 2. MSEs of the H_2, H_4 and the HAF versus SNR for a quadratic FM signal.

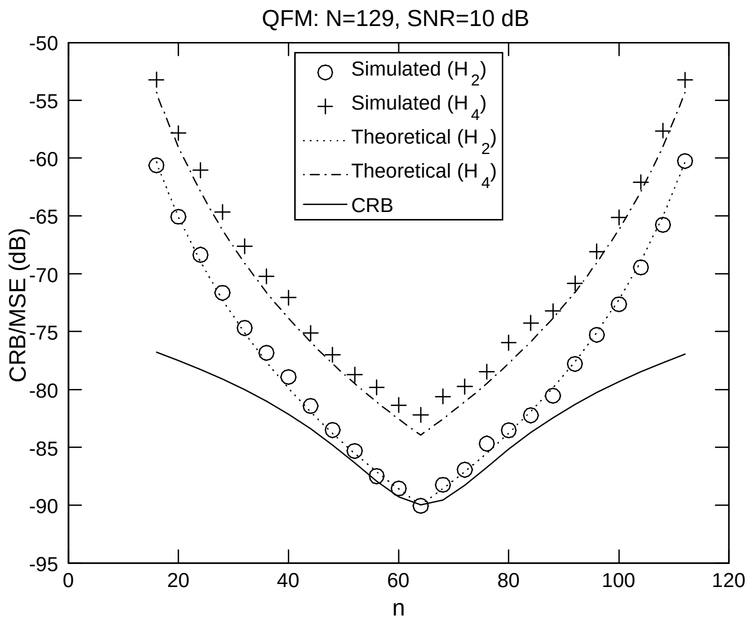

Fig. 3. MSEs of various HPFs versus time n for a quadratic FM signal.

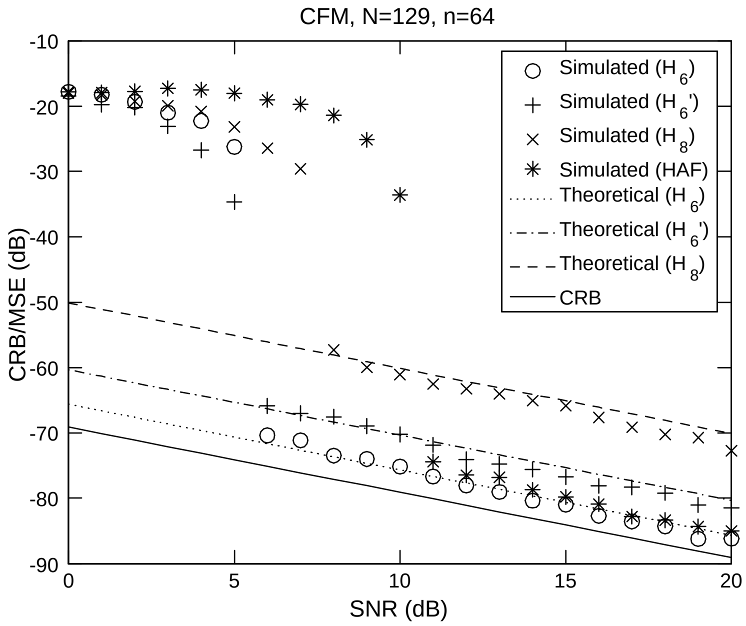

Fig. 4. MSEs of various HPFs and the HAF versus SNR for a cubic FM signal.

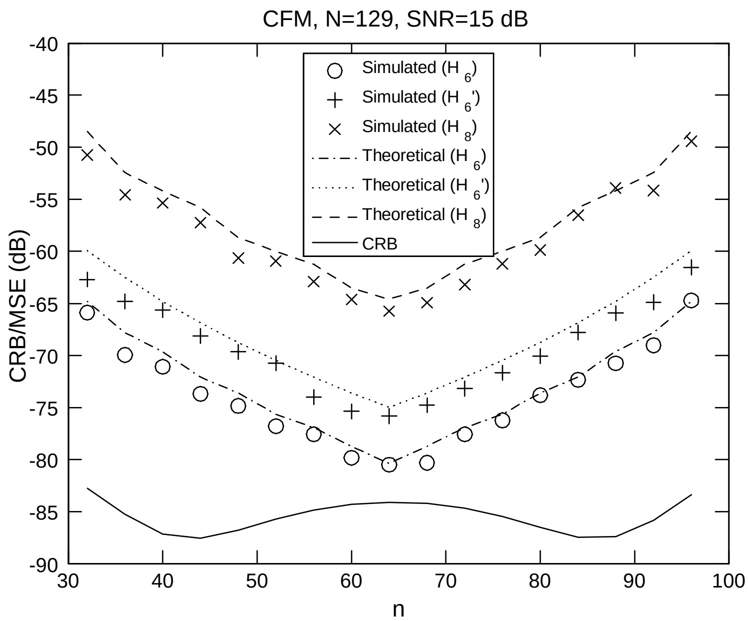

Fig. 5. MSEs of various HPFs versus time n for a cubic FM signal.

the IFR is estimated at $n = 64$. The results verify again that our theoretical MSEs agree well with the simulations for the H_6, H_6' and H_8-based methods at high SNR. We note that the H_6-based estimator provides the minimum MSE among the three. Moreover, the two sixth-order HPF H_6 and H_6' show a lower SNR threshold than that of the eighth-order HPF H_8. Comparison with the HAF-based estimator shows that the HAF-based estimator can generate good performance at SNRs above 11 dB, but its SNR threshold is higher than the HPF-based methods.

Fig. 5 plots the MSEs of the three HPF-based estimators with the maximum window length $M_{\max}$ in (13) versus time n when SNR $= 15$ dB. It is observed that, even at the middle point, the MSE of the three IFR estimators cannot reach the CRB. Once again, the simulated MSEs match the theoretical results. From Figs. 4 and 5, it is seen that the best HPF for the cubic FM signal is H_6 in terms of either the MSEs or the SNR threshold.

V. Conclusion

This paper has presented a generalized performance analysis of the HPF-based IFR estimators in terms of their asymptotic bias and MSE for the estimation of polynomial phase signals with an arbitrary order. The results show that the MSE of the IFR estimate is proportional to the sum of squared multiplicity of the HPF coefficients, and inversely proportional to the SNR and the window length. Both exact and asymptotic CRBs for the IFR estimation have been established. Two examples have been provided to show that our results are consistent with the existing results for the cases of $p = 2$ and $p = 3$. Numerical examples have been given to verify the analytical results.

Appendices

I. Approximation of $K_x(n,m)$ at High SNR

By applying the HPF to the above noisy PPS signal, the nonlinear kernel of the HPF in discrete form can be expressed as

$$K_x(n,m) = \prod_{i=1}^{L} [s(n+d_im)+v(n+d_im)]^{(r_i)k_i} \times [s(n-d_im)+v(n-d_im)]^{(r_i)k_i}, \qquad (24)$$

where L is the number of different coefficients d_i and r_i, k_i, is the multiplicity of the coefficients d_i and r_i, and $\sum_{i=1}^{L} k_i = q/2$.

Using the binomial expansion

$$[s(n+d_im)+v(n+d_im)]^{(r_i)k_i} = \sum_{\ell=0}^{k_i} \binom{k_i}{\ell} v^{(r_i)\ell}(n+d_im) s^{(r_i)[k_i-\ell]}(n+d_im) \qquad (25)$$

and a similar expansion for $[s(n-d_im)+v(n-d_im)]^{(r_i)k_i}$, we can rewrite (24) as follows

$$\begin{aligned} K_x(n,m) &= \\ &= \prod_{i=1}^{L} s^{(r_i)k_i}(n+d_im) s^{(r_i)k_i}(n-d_im) \\ &\times \Bigg[\sum_{\ell_1=0}^{k_i} \sum_{\ell_2=0}^{k_i} \binom{k_i}{\ell_1} \binom{k_i}{\ell_2} v^{\ell_1}(n+d_im) \\ &\quad v^{\ell_2}(n-d_im) s^{-\ell_1}(n+d_im) s^{-\ell_2}(n-d_im) \Bigg]^{(r_i)} \\ &\approx \prod_{i=1}^{L} s^{(r_i)k_i}(n+d_im) s^{(r_i)k_i}(n-d_im) \\ &\times \big[1 + k_i v(n-d_im) s^{-1}(n-d_im) \\ &+ k_i v(n+d_im) s^{-1}(n+d_im)\big]^{(r_i)}, \end{aligned} \qquad (26)$$

where the approximation is due to the high SNR assumption which allows us to ignore the high-order noise terms. Decomposing (26) into signal-only terms and noise-related terms, we have

$$
\begin{aligned}
&K_x(n,m) \approx \\
&\approx \left\{ \prod_{i=1}^{L} \left[s^{k_i}(t+d_i\tau) s^{k_i}(t-d_i\tau) \right]^{(r_i)} \right\} \\
&\times \left\{ 1 + \sum_{i=1}^{L} k_i \left[v(n-d_i m) s^{-1}(n-d_i m) \right.\right. \\
&\left.\left. + v(n+d_i m) s^{-1}(n+d_i m) \right]^{(r_i)} \right\} \\
&= K_s(n,m) + K_s(n,m) \\
&\times \sum_{i=1}^{L} k_i \left[v(n+d_i m) s^{-1}(n+d_i m) \right. \\
&\left. + v(n-d_i m) s^{-1}(n-d_i m) \right]^{(r_i)},
\end{aligned}
$$

which is (10).

II. First-Order Perturbation Method

The basic principle of the first-order permutation method is shown as follows. Assume that $g_N(\omega)$ is a complex function depending on a real variable ω and on an integer N. The squared-magnitude of $g_N(\omega)$ has a global maximum at $\omega = \omega_0$. Suppose a random function $\delta g_N(\omega)$ moves the global maximum of $g_N(\omega)$ from the nominal ω_0 by $\delta\omega$, the first-order approximation for $\delta\omega$ is $\delta\omega \approx -\beta/\alpha$ [14], where

$$
\begin{aligned}
\alpha = 2\Re\left\{ g_N(\omega_0) \frac{\partial^2 g_N^*(\omega_0)}{\partial \omega^2} \right\} + \\
+ 2\Re\left\{ \frac{\partial g_N(\omega_0)}{\partial \omega} \frac{\partial g_N^*(\omega_0)}{\partial \omega} \right\},
\end{aligned} \tag{27}
$$

and

$$
\begin{aligned}
\beta = 2\Re\left\{ g_N(\omega_0) \frac{\partial \delta g_N^*(\omega_0)}{\partial \omega} \right\} + \\
+ 2\Re\left\{ \frac{\partial g_N(\omega_0)}{\partial \omega} \delta g_N^*(\omega_0) \right\},
\end{aligned} \tag{28}
$$

where $\Re(\cdot)$ represents the real part of $(\cdot)$. The mean-square value of $\delta\omega$ is given by

$$
E\{(\delta\omega)^2\} \approx \frac{E\{\beta^2\}}{\alpha^2}, \tag{29}
$$

where $E\{\cdot\}$ denotes the expectation.

III. Asymptotic Analysis of the HPF-based Estimator

The HPF of a noise-free PPS $s(n)$ is

$$
\mathrm{H}_s(n,\omega) = \sum_{m=-M}^{M} K_s(n,m) e^{-j\omega m^2}. \tag{30}
$$

By choosing the HPF coefficients according to *Proposition 1*, the HPF attains the maximum at $\omega_0 = \Omega(n)$.

To derive its asymptotic MSE of the HPF-based IFR estimate, we first determine the complex function $g_N(\omega)$ and its random perturbation $\delta g_N(\omega)$ for a specific n. According to the results in Appendix A, $g_N(\omega)$ and $\delta g_N(\omega)$ can be expressed as

$$
\begin{aligned}
g_N(\omega) &= \sum_{m=-M}^{M} K_s(n,m) e^{-j\omega m^2}, \\
\delta g_N(\omega) &= \sum_{m=-M}^{M} K_v(n,m) e^{-j\omega m^2},
\end{aligned} \tag{31}
$$

where $K_v(n,m)$ is given in (10). For simplicity, we drop the index n in the above functions. Since

$$
K_s(n,m) = A^q e^{j\left(\omega_0 m^2 + \varsigma\right)}, \tag{32}
$$

the functions $g_N(\omega), \delta g_N(\omega)$, and their derivatives, evaluated at the global maximum $\omega_0 = \Omega(n)$, are given by

$$
\begin{aligned}
g_N(\omega_0) &= A^q e^{j\varsigma} (2M+1) \\
\frac{\partial g_N(\omega_0)}{\partial \omega} &= -j \frac{A^q e^{j\varsigma}}{3} M(M+1)(2M+1), \\
\frac{\partial^2 g_N(\omega_0)}{\partial \omega^2} &= -\frac{A^q e^{j\varsigma}}{15} M(M+1) \\
&\quad \times (2M+1)\left(3M^2+3M-1\right), \\
\delta g_N^*(\omega_0) &= A^q e^{-j\varsigma} \sum_m z_{vs}(n,m), \\
\frac{\partial \delta g_N^*(\omega_0)}{\partial \omega} &= j A^q e^{-j\varsigma} \sum_m m^2 z_{vs}(n,m),
\end{aligned}
$$

where

$$
\begin{aligned}
z_{vs}(n,m) = \sum_{i=1}^{L} k_i & \left[v(n+d_i m) s^{-1}(n+d_i m) \right. \\
& \left. + v(n-d_i m) s^{-1}(n-d_i m) \right]^{(-r_i)},
\end{aligned} \tag{33}
$$

and $(\cdot)^{(-r_i)}$ means the conjugate of $(\cdot)^{(r_i)}$.

By inserting the above intermediate results into (27) and (28), we obtain

$$\begin{aligned}\alpha &= -\frac{2A^{2q}}{45} M(M+1)(2M-1) \\ &\quad \times (2M+1)^2 (2M+3), \\ \beta &= 2A^{2q}(2M+1)\Im[\Gamma],\end{aligned} \tag{34}$$

where $\Im[\cdot]$ represents the imaginary part of $[\cdot]$ and

$$\Gamma = \sum_m \left(m^2 - \frac{M(M+1)}{3}\right) z_{vs}(n,m). \tag{35}$$

Therefore, the first-order approximation of the perturbation on the maximum point $\delta\omega$ is

$$\delta\omega = \frac{45\Im[\Gamma]}{M(M+1)(2M-1)(2M+1)(2M+3)}. \tag{36}$$

Taking the expectation of (36) with respect to $v(n)$, we can verify, from (33) and (36), that $E\{z_{vs}(n,m)\} = 0$, and, hence,

$$E\{\delta\omega\} = 0. \tag{37}$$

In other words, the estimator is asymptotically unbiased.

According to (29), we need to compute $E\{\beta^2\}$ in order to find the asymptotic variance. From (34),

$$\begin{aligned}E\{\beta^2\} =& 2A^{4q}(2M+1)^2 \Re \\ &\times [E\{\Gamma\Gamma^*\} - E\{\Gamma\Gamma\}],\end{aligned} \tag{38}$$

where we use the fact that

$$E\{\Im[x]\Im[y]\} = 0.5\Re[E\{xy^*\} - E\{xy\}].$$

From (35), we have

$$\begin{aligned}E\{\Gamma\Gamma^*\} =& \sum_{m_1}\sum_{m_2}\left(m_1^2 - \frac{M(M+1)}{3}\right) \\ &\times \left(m_2^2 - \frac{M(M+1)}{3}\right) \\ &\times E\{z_{vs}(n,m_1) z_{vs}^*(n,m_2)\}\end{aligned} \tag{39}$$

$$\begin{aligned}E\{\Gamma\Gamma\} =& \sum_{m_1}\sum_{m_2}\left(m_1^2 - \frac{M(M+1)}{3}\right) \\ &\times \left(m_2^2 - \frac{M(M+1)}{3}\right) \\ &\times E\{z_{vs}(n,m_1) z_{vs}(n,m_2)\}.\end{aligned} \tag{40}$$

Using (41) to evaluate $E\{z_{vs}(n,m_1) z_{vs}^*(n,m_2)\}$ and $E\{z_{vs}(n,m_1) z_{vs}(n,m_2)\}$ results in

$$\begin{aligned}&E\{z_{vs}(n,m_1) z_{vs}^*(n,m_2)\} \approx \\ &\approx 2\sigma^2 A^{-2} \sum_{i=1}^{L} (k_i)^2 \delta(m_1 \pm m_2), \\ &E\{z_{vs}(n,m_1) z_{vs}(n,m_2)\} \approx 0,\end{aligned}$$

where we used the fact that $d_i \neq d_j$ and $r_i \neq r_j$ if $i \neq j$. Inserting these intermediate results into (38), (39) and (40) yields

$$\begin{aligned}E\{\beta^2\} =& \frac{8A^{4q-2}\sigma^2 \sum_{i=1}^{n_1} (k_i)^2}{45} M(M+1) \\ &\times (2M-1)(2M+1)^3(2M+3).\end{aligned} \tag{41}$$

Combining (29), (34) and (41), the variance of $\delta\omega$ is given by eq. 42, where $\mathrm{SNR} = A^2/\sigma^2$.

References

[1] A. W. Rihaczek, *Principles of high-resolution radar.* New York: McGraw-Hill, 1969.

[2] B. Porat, *Digital processing of random signals: theory and methods.* Englewood Cliffs, NJ: Prentice Hall, 1994.

[3] P. O'Shea, "A new technique for estimating instantaneous frequency rate," *IEEE Signal Processing Lett.*, vol. 9, no. 8, pp. 251–252, August 2002.

[4] T. Abotzoglou, "Fast maximum likelihood joint estimation of frequency and frequency rate," *IEEE Trans. Aerosp. Electron. Syst.*, vol. 22, pp. 708–715, November 1986.

$$E\{(\delta\omega)^2\} = \frac{90\sum_{i=1}^{L}(k_i)^2}{\text{SNR}M\,(M+1)\,(2M-1)\,(2M+1)\,(2M+3)}, \tag{42}$$

[5] S. Barbarossa, A. Scaglione, and G. Giannakis, "Product high-order ambiguity function for mulit-component polynomial phase signal modeling," *IEEE Trans. Signal Processing*, vol. 46, no. 3, pp. 691–708, March 1998.

[6] S. Barbarossa and A. Scaglione, "Autofocusing of SAR images based on the product high-order ambiguity function," *IEE Proc.-Radar Sonar Navig.*, vol. 145, no. 5, pp. 269–273, October 1998.

[7] J. J. Sharma, C. H. Gierull, and M. J. Collins, "The influence of target acceleration on velocity estimation in dual-channel SAR-GMTI," *IEEE Trans. Geoscience and Remote Sensing*, vol. 44, no. 1, pp. 134–147, January 2006.

[8] ——, "Compensating the effects of target acceleration in dual-channel SAR-GMTI," *IEE Proc.-Radar Sonar Navig.*, vol. 153, no. 1, pp. 53–62, February 2006.

[9] V. Katkovnik, "Nonparametric estimation of instantaneous frequency," *IEEE Trans. Information Theory*, vol. 43, no. 1, pp. 183–189, January 1997.

[10] P. O'Shea, "A fast algorithm for estimating the parameters of a quadratic FM signal," *IEEE Trans. Signal Processing*, vol. 52, no. 2, pp. 385–393, February 2004.

[11] B. Porat and B. Friedlander, "Asymptotic statistical analysis of the high-order ambiguity function for parameter estimation of polynomial-phase signals," *IEEE Trans. Info. Theory*, vol. 42, no. 3, pp. 995–1001, May 1996.

[12] P. Wang, I. Djurović, and J. Yang, "Generalized high-order phase function for parameter estimation of polynomial phase signal," *IEEE Trans. Signal Processing*, vol. 56, no. 7, pp. 3023–3028, July 2008.

[13] B. Barkat and B. Boashash, "Instantaneous frequency estimation of polynomial FM signals using the peak of the PWVD: Statistical performance in the presence of additive Gaussian noise," *IEEE Trans. Signal Processing*, vol. 47, no. 9, pp. 2480–2490, September 1999.

[14] S. Peleg and B. Porat, "Linear FM signal parameter estimation from discrete-time observations," *IEEE Trans. Aerosp. Electron. Syst.*, vol. 27, no. 4, pp. 607–614, July 1991.

[15] ——, "The Cramer-Rao lower bound for signals with constant amplitude and polynomial phase," *IEEE Trans. Signal Processing*, vol. 39, no. 3, pp. 749–752, March 1991.

[16] S. M. Kay, *Fundamental of Statistical Signal Processing: Estimation Theory.* Upper Saddle River, NJ: Prentice Hall, 1998.

[17] B. Ristic and B. Boashash, "Comments on "the Cramer-Rao Lower Bounds for signals with constant amplitude and polynomial phase"," *IEEE Trans. Signal Processing*, vol. 46, no. 6, pp. 1708–1709, June 1998.